Clinical Neurophysiology 130 (2019) 180–188

Contents lists available at ScienceDirect

Clinical Neurophysiology

journal homepage: www.elsevier.com/locate/clinph

# Multifocal visual evoked potentials and contrast sensitivity correlate with ganglion cell-inner plexiform layer thickness in multiple sclerosis

Divya Narayanan [a], Han Cheng [a,*], Rosa A. Tang [b], Laura J. Frishman [a]

[a] College of Optometry, University of Houston, Houston, TX, USA
[b] University of Houston, MS Eye CARE Clinic, Houston, TX, USA

See Editorial, pages 157–159

ARTICLE INFO

*Article history:*
Accepted 5 October 2018
Available online 13 November 2018

*Keywords:*
Multiple sclerosis
Remyelination
Visual function
Multifocal visual evoked potential
Contrast sensitivity
Optic neuritis

HIGHLIGHTS

- MfVEP amplitude is more highly correlated with GCIPL than RNFL thickness in ON.
- GCIPL is a strong structural biomarker for optic nerve degeneration in RRMS.
- MfVEP is more sensitive than OCT in detecting subclinical defects in non-ON.

ABSTRACT

*Objective:* To examine the relationship between optical coherence tomography (OCT) macular ganglion cell-inner plexiform layer thickness (GCIPLT), peripapillary retinal nerve fiber layer thickness (RNFLT) and visual function in relapsing-remitting multiple sclerosis (RRMS).
*Methods:* Cirrus OCT, VERIS 60-sector multifocal visual evoked potential (mfVEP) and Pelli-Robson contrast sensitivity (CS) were obtained for 53 eyes with last optic neuritis (ON) > 6 months and 105 non-ON eyes in 90 patients. One eye (43 ON, 73 non-ON) was used for correlations when both had the same history. Global (G, 60 sectors) and central 5.6° (C, 24 sectors) mfVEP amplitude and latency were calculated as mean logSNR and median latency.
*Results:* Eyes showing abnormal mfVEP (amplitude or latency) vs OCT (GCIPLT or RNFLT) was 77% vs 69% ($p = 0.33$) in ON, 45% vs 22% ($p < 0.0005$) in non-ON. In ON and non-ON, mfVEP measures and CS correlated with GCIPLT and RNFLT ($r = -0.24$ to 0.78, $p = 0.03$–$0.0001$). In ON, mfVEP amplitude (C,G) correlated better with GCIPLT ($r = 0.78, 0.76$) than RNFLT ($r = 0.43, 0.58$; $p < 0.001, 0.01$).
*Conclusions:* MfVEP measures and CS correlated well with GCIPLT and RNFLT in ON and non-ON. MfVEP amplitudes were more highly correlated with GCIPLT than RNFLT in ON. MfVEP detected significantly more defects than OCT in non-ON.
*Significance:* GCIPLT, mfVEP and CS provide useful measures of optic nerve integrity in RRMS.


## 1. Introduction

Neurodegeneration is an important component of the pathological process in multiple sclerosis (MS), a chronic disease of the central nervous system (CNS). The anterior visual pathway, a small compartment within the CNS, is a prominent site of demyelination and neurodegenerative damage and serves as a good model in MS (Pisa et al., 2017, Toosy et al., 2017). It is well known that within the first 3–6 months following acute optic neuritis (ON), significant axonal and neuronal loss occurs (Costello et al., 2008, Syc et al., 2012), resulting in permanent visual dysfunction. MS eyes, even without a history of optic neuritis (non-ON eyes) can have significant abnormalities in structure (Green et al., 2010, Narayanan et al., 2014) and in visual function (Brusa et al., 1999, Laron et al., 2009, Wang et al., 2012). Furthermore significant changes in both structural and functional measures occur over time in 'clinically-silent' MS eyes with or without a history of ON (Narayanan et al., 2014, Narayanan et al., 2015a).

* Corresponding author at: College of Optometry, University of Houston, 4901 Calhoun Rd, Houston, TX 77204-2020, USA. Fax: +1 713 743 2053.
*E-mail address:* hcheng@central.uh.edu (H. Cheng).

https://doi.org/10.1016/j.clinph.2018.10.007
1388-2457/

Spectral-domain optical coherence tomography (OCT) has emerged as a sensitive technique to assess thickness changes from discrete retinal layers in MS eyes (Petzold et al., 2017). Recent studies suggest that compared to peripapillary retinal nerve fiber layer (RNFL) thickness (RNFLT), macular ganglion cell-inner plexiform layer (GCIPL) thickness (GCIPLT) can be more selective in quantifying and tracking neurodegeneration in MS as it is less confounded by gliosis and edema found in the RNFL (Green et al., 2010, Saidha et al., 2011, Ratchford et al., 2013, Gonzalez-Lopez et al., 2014, Narayanan et al., 2014, Kupersmith et al., 2016, Britze et al., 2017, Pietroboni et al., 2017).

The multifocal visual evoked potential (mfVEP) is a non-invasive test that provides topographic measures of visual function from focal regions (Hood and Greenstein, 2003). MfVEP response amplitude and latency informs about axonal and myelin integrity respectively (Graham and Klistorner, 2017). MfVEP has high sensitivity in detecting visual deficits (Ruseckaite et al., 2005, Grover et al., 2008, Laron et al., 2010), can detect more abnormalities than traditional pattern-reversal VEP in MS/ON eyes (Klistorner et al., 2008b, Pihl-Jensen et al., 2017), and can be reliably used to track visual function changes over time in MS eyes (Yang et al., 2007, Narayanan et al., 2015b).

Recent studies have highlighted the need for novel neuroprotective and remyelinating therapies to limit or halt neurodegenerative processes in MS (Maghzi et al., 2013). Since structural and functional measures from OCT and mfVEP can offer complementary information on the integrity of the visual pathway (Laron et al., 2010), both could potentially be used to assess therapeutic effects of new treatment strategies. Previous findings on the structure-function relationship in MS are not always consistent, with better correlation of visual function with GCIPLT than with RNFLT reported by some (Saidha et al., 2011, Seigo et al., 2012, Walter et al., 2012) but not others (Sriram et al., 2014).

To our knowledge, currently the only publication that investigated the relationship between mfVEP responses and GCIPLT was limited to MS non-ON eyes (Sriram et al., 2014, Pihl-Jensen et al., 2017). In the current study, we evaluated the relationship between structural measurements (GCIPLT and RNFLT) and functional tests including mfVEP amplitude and latency, Pelli-Robson contrast sensitivity (CS), and Humphrey visual field (HVF) in eyes with or without a history of ON from relapsing-remitting MS (RRMS) patients. Some of the findings in this study have been reported in abstract form (Narayanan D, et al. *Invest Ophthalmol Vis Sci* 2014; 55: E-Abstract 5777, Narayanan D, et al, *Int J MS Care* 2014; Volume 16, Supplement 3).

## 2. Methods

### 2.1. Subjects

All RRMS patients were recruited from the University of Houston MS Eye CARE clinic and underwent comprehensive eye exams by an experienced neuro-ophthalmologist. Patients with systemic abnormalities such as diabetes or other ocular abnormalities such as glaucoma, retinal diseases, refractive errors greater than 6 D or MS eyes with an ON attack within 6 months (acute ON) of the exam date were excluded. OCT, mfVEP, and Pelli-Robson CS were obtained from 90 RRMS patients (mean age 40.5 ± 10.5 years, mean MS duration since diagnosis 6.5 ± 7.4 years). All patients were fully ambulatory. Included for analysis were 105 MS eyes with no previous history of ON (non-ON eyes) and 53 ON eyes with last ON > 6 months (mean time elapsed from last ON 3.8 ± 5.0 years) (Table 1). A total of 22 eyes were excluded (18 eyes with acute ON < 6 months, 3 eyes with OCT signal strength < 7, and 1 eye with poor centration on OCT imaging). Among those included, 44 ON and 88 non-ON eyes also had reliable HVF 24–2 or 30–2 tests (see criterion below).

**Table 1**
Demographic and clinical characteristics.

| | | |
|---|---|---|
| Age (years, mean ± SD) | 40.5 ± 10.5 | |
| F:M | 5.9:1 | |
| MS duration since diagnosis (years, mean ± SD) | 6.5 ± 7.4 | |
| | ON (n = 53) | Non-ON (n = 105) |
| Eyes with acuity 20/20 or better (%) | 40 (75%) | 100 (95%) |
| Time since last ON (years, mean ± SD) | 3.8 ± 5.0 | N/A |

All procedures adhered to the tenets of Declaration of Helsinki. The protocol was approved by the University of Houston Committee for the Protection of Human Subjects. Informed consent was obtained from all subjects.

### 2.2. Optical coherence tomography (OCT)

OCT was performed using Cirrus-HD OCT 4000 version 6.5 (Carl Zeiss Meditec, Inc., Dublin, CA). Macular GCIPLT was obtained using the Macular Cube 512 × 128 A-scan protocol that images a 6 × 6 mm area centered at the fovea. The GCIPLT was derived automatically by the machine software over an elliptical annulus (2.4 × 2.0 mm horizontal and vertical radius) excluding the central foveal region (0.6 × 0.5 mm radius). Peripapillary RNFLT was measured using the Optic Disc Cube 200 × 200 A-scan protocol that images the disc in a 6 × 6 mm region. Only images with signal strength ≥7, good centration and no erroneous segmentation upon visual inspection were included. Average GCIPLT, average RNFLT and temporal quadrant RNFLT (the quadrant receiving most of the macular fibers) were included for analysis.

### 2.3. Pelli-Robson contrast sensitivity (CS)

Monocular CS was assessed using the Pelli-Robson CS chart at 1 m. The chart comprises 16 triplets of letters each subtending 2.8°. Letters within a triplet have the same contrast and successive triplets decrease in contrast from 0 to 2.25 log units in 0.15 steps. Each letter read correctly was counted as 0.05 log unit and the test was terminated when a subject missed 2 letters in a triplet. Our lab established normative value was 1.6 ± 0.1 out of a theoretically possible score of 2.40 (Narayanan et al., 2015b). Please note that all log values in this paper denote $\log_{10}$.

### 2.4. Multifocal visual evoked potential (mfVEP)

MfVEP was recorded and analyzed using methods established by Hood and Greenstein (2003), Fortune et al. (2004), Hood et al. (2004a,b) and has been described in detail in our prior studies (Laron et al., 2009, Narayanan et al., 2015a). Briefly, the stimulus (VERIS 5.1) was a 60 sector cortically-scaled dartboard pattern (mean luminance 66 cd/m$^2$, contrast 95%) (Fig. 1a). Each sector contained 16 checks (8 white and 8 black) that reversed in contrast following a pseudorandom m-sequence (frame rate 75 Hz, 13.3 ms per m-step, m = $2^{15}$-1). Three channels were recorded with the following electrode placement (approximate locations by International 10-10 system also given) (American Clinical Neurophysiology Society, 2006): a ground on the forehead (Fpz), a reference on the inion, 3 active electrodes with one placed 4 cm above the inion (near Oz), and two placed 1 cm above and 4 cm on either side of the inion (near O9 and O10). Two 7-minute recordings from each eye were obtained and averaged after the first slice of the second-order kernel from each channel was exported from VERIS. This averaging and all analyses were

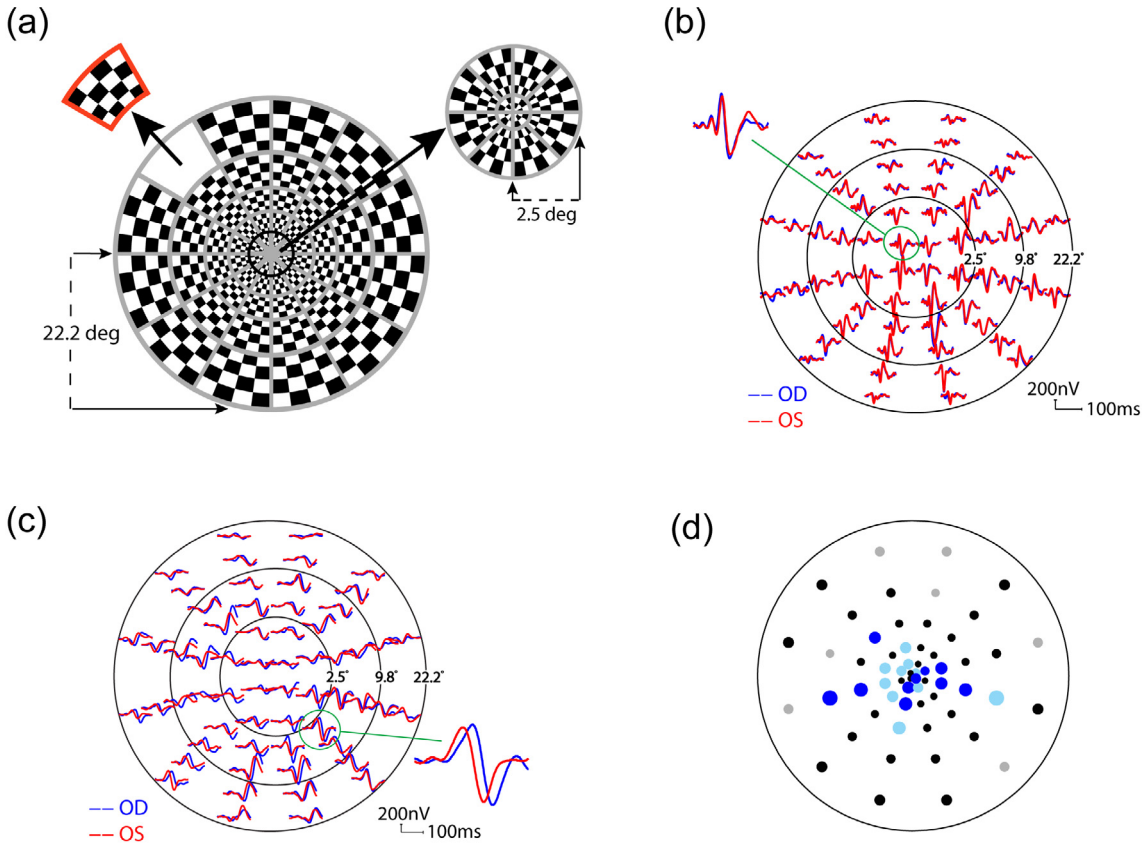


**Fig. 1.** (a) The mfVEP stimulus contains 60 sectors of black and white checks (one sector shown in red). (b) The mfVEP responses from the right eye (blue) and the left eye (red) of a normal subject are essentially identical. (c) The mfVEP responses from an MS subject show prolonged latencies in the right eye (blue) compared to those from the left eye (red). (d) The interocular latency probability plot shows a cluster of prolonged latencies in the right eye (dark blue for $p < 0.01$, light blue for $p < 0.05$) compared to the left eye of an MS patient who had an ON attack in the right eye two years prior and no history of ON in the left eye. Black symbols denote no significant differences compared to the Portland normative database, small gray symbols for responses too small for comparisons (Hood and Greenstein, 2003, Fortune et al., 2004, Hood et al., 2004b).

performed using a customized MATLAB (Mathworks Inc, MA.) software from Hood and colleagues. The software mathematically derived responses from three additional channels and all responses went through a low-pass filter with a sharp cut-off of 35 Hz (a Fourier transform technique). For each stimulus sector, the response amplitude from each channel was measured by the signal to-noise ratio (SNR) calculated as the root-mean-square (RMS) amplitude of the sector's response in the signal window (45–150 ms) divided by the mean RMS from the noise windows (325–430 ms) of all 60 sectors. The largest SNR from the 6 channels was selected for each sector to compose the 60 "best channel" responses for that eye (Fig. 1b, c), which were used for further analysis as shown below. The response latency for a sector was measured as the temporal shift (in milliseconds) producing the best cross-correlation between the sector's waveform and a corresponding normative template previously established from 100 normal subjects (Fortune et al., 2004, Hood et al., 2004a). In the current study, mfVEP response amplitude and latency were calculated as mean logSNR and median latency from all 60 sectors for global and central 24 sectors for 5.6° region. The central 5.6° radius of mfVEP stimulus (7.3° horizontal and 6.0° vertical, when scaled for retinal ganglion cell displacement (Drasdo et al., 2007) corresponds quite well to the GCIPLT region measured by Cirrus OCT (8° horizontal and 6.7° vertical radius).

For each eye, the software also displays four 60-sector probability plots (monocular amplitude, interocular amplitude, monocular latency, interocular latency) that are analogous to the HVF total deviation plots. On each probability plot, responses from individual sectors were compared to the Portland normative data from 100 eyes (Fortune et al., 2004), and marked as normal (black dots) or abnormal (colored dots with saturated colors for $p < 0.01$ and unsaturated colors for $p < 0.05$) (Hood and Greenstein, 2003, Fortune et al., 2004, Hood et al., 2004a,b). To define whether an eye had abnormal mfVEP amplitude or latency, we examined monocular and interocular probability plots for the presence of abnormal clusters (adjacent abnormal sectors, Fig. 1d) that met our previously established cluster criteria with 95% specificity (Laron et al., 2009).

### 2.5. Humphrey visual fields (HVF)

Visual fields were tested using the Humphrey visual field analyzer 750 (Carl Zeiss Meditec, Inc.) with 24-2 or 30-2 SITA (Swedish interactive threshold algorithm) protocols and additionally 10-2 in some patients. A HVF test was considered unreliable and not included for analysis if fixation loss, false positives or false negatives were >33%. For each eye, the mean deviation (MD) was recorded in dB. In addition, for each eye, individual deviations from the total deviation plot (HVF 24-2, 30-2 or 10-2) were unlogged and averaged to calculate relative visual sensitivity (RVS) (Cheng et al., 2007).

### 2.6. Statistics (Stata 14)

Group means were compared using two sample $t$ test (no change in results when Generalized Estimating Equation was used to account for age and intra-subject inter-eye correlation). Effect size between the means of ON or non-ON and normal was

measured by Cohen's d. McNemar's test was used for comparing two correlated proportions. Correlation between structural and functional measures was assessed using Pearson's correlation for ON and non-ON eyes separately. For each group (ON or non-ON), only one eye from each subject was included for correlation analyses to ensure independent samples. Stata cortesti was used for comparing correlation coefficients (accessed the website on 1/3/2018 http://fmwww.bc.edu/RePEc/bocode/c/cortesti.html). Additionally, multiple linear regression was used to control age, disease duration, and other covariates for assessing partial correlation between various structural-functional parameters. For multiple comparisons, Bonferroni correction was used to adjust the $p$ values and control family-wise error. Two-tailed $p$ values were reported with $p < 0.05$ considered as significant.

## 3. Results

The group means of OCT, mfVEP and CS measurements in 53 ON and 105 non-ON eyes from 90 RRMS patients are summarized in Table 2, mean MD of those with reliable HVF 24-2/30-2 (44 ON, 88 non-On eyes) was also included. All mean values (GCIPLT, RNFLT, mfVEP amplitude, latency, CS, HVF MD) were worse in ON than non-ON or normal eyes ($p = 0.02$ for HVF MD ON vs non-ON, $p < 0.0001$ for all others). Mean values in non-ON were worse than their respective normative values for GCIPLT, HVF MD ($p < 0.0001$ for both), mfVEP amplitude ($p = 0.02$) and latency ($p < 0.001$) (Laron et al., 2009, Mwanza et al., 2011a, Wall et al., 2013, Narayanan et al., 2015b). Cohen's d shows the standardized difference between the means of ON or non-ON and normal groups. Area under the curve (AUC) for the receiver operating characteristic (ROC) using mfVEP amplitude, latency and CS was 0.84, 0.75, 0.79 respectively in ON; 0.61, 0.61, 0.51 in non-ON.

As shown in Table 3, the percentage of MS eyes showing abnormal (below 5% of the machine-norm) GCIPLT, RNFL or temporal RNFLT was 60%, 52%, 44% respectively in ON, 19%, 11%, 13% in non-ON; among them GCIPLT vs temporal RNFLT (60% vs 44%) in ON, GCIPLT vs RNFLT (19% vs 11%) in non-ON showed a trend toward statistical significance (two-tailed $p = 0.06$ for both). For mfVEP, cluster analysis (95% specificity) of the probability plots (see Methods and Fig. 1d) revealed abnormal amplitude and latency in 60% and 57% of ON eyes respectively, 24% and 30% of non-ON eyes. In ON, 77% vs 69% ($p = 0.33$) eyes showed abnormality in mfVEP (amplitude or latency) vs OCT (GCIPLT or RNFLT), with a total of 89% eyes showing defects in either mfVEP or OCT. In non-ON, more eyes showed abnormality for mfVEP (45%) than OCT (22%, $p < 0.0005$), and a total of 54% showed either defect. For CS, 40% ON and 9% non-ON had CS below 5% of the normative values.

Relationships between structural measures (GCIPLT, RNFLT) and various measures of visual function (CS, HVF RVS, mfVEP amplitude, latency) were assessed using Pearson's correlation. For this analysis, only one eye was chosen when both eyes had the same history to ensure independence resulting in a total of 43 ON, 73 non-ON eyes for OCT, mfVEP and CS; 36 ON and 66 non-ON eyes for HVF 24-2 or 30-2, 15 ON and 10 non-ON eyes for HVF 10-2. In addition to global mean values, mfVEP responses from the central 5.6° stimulus were specifically used for correlation with GCIPLT in order to match the GCIPLT region (after consideration of RGC displacement) scanned by OCT (see Methods). Temporal quadrant RNFLT was used for correlation with mfVEP central 5.6° responses.

Pearson's correlation and $p$ values are summarized in Table 4. Representative scatter plots are shown in Figs. 2 and 3. In ON eyes, all functional measures correlated significantly with GCIPLT ($r = -0.40$–$0.78$, $p = 0.03$–$0.0001$) while CS, mfVEP amplitude and latency ($r = -0.33$–$0.61$, $p = 0.03$–$0.0001$) but not HVF RVS correlated significantly with RNFLT. In non-ON eyes, all functional measures except HVF RVS showed significant correlation with GCIPLT and RNFLT ($r = -0.24$–$0.51$, $p = 0.04$–$0.0001$).

In ON eyes, mfVEP amplitude showed stronger correlation with GCIPLT ($r = 0.78$, 0.76 for central and global amplitude) than RNFLT ($r = 0.43$, 0.58; $p < 0.001$, 0.01 after Bonferroni correction for central and global amplitude). When multiple linear regression was used to control for age, disease duration and RNFLT, the following parameters retained their significant correlation with GCIPLT: mfVEP amplitude in ON and non-ON eyes (partial $r = 0.78$, 0.51 for central and global amplitude in ON, partial $r = 0.43$, 0.39 for central and global in non-ON; $p < 0.001$ for all), mfVEP central latency (partial $r = -0.42$), CS (partial $r = 0.51$) and 24-2/30-2 RVS (partial $r = 0.42$) in ON eyes ($p = 0.02$ for all); however, when age, disease duration and GCIPLT were controlled, none of the functional measurements correlated with RNFLT ($p > 0.05$ for all).

Compared to latency, global/central mfVEP amplitude in ON and central amplitude in non-ON correlated more strongly with GCIPLT ($p < 0.05$ for all), however, such statistical significance did not hold after Bonferroni correction was applied. When multiple linear regression was used to control covariates (age, MS duration, mfVEP amplitude or latency), mfVEP amplitude retained significant correlation with GCIPLT (partial $r = 0.68$ central, 0.72 global in ON; partial $r = 0.46$ central, 0.48 global in non-ON, $p < 0.0001$ for all) and RNFLT (partial $r = 0.54$ in ON, $p = 0.0005$) whereas latency no longer correlated with GCIPLT or RNFLT.

## 4. Discussion

Recent OCT studies of acute ON have suggested that GCIPLT may be a better biomarker for structural damage than peripapillary RNFLT (Kupersmith et al., 2016). Our study concurs with this idea

**Table 2**
Group mean (±SE) and Cohen's d (95% confidence interval) for difference between ON or non-ON and normal for various measurements.

| | Normal | ON | Cohen's d | Non-ON | Cohen's d |
|---|---|---|---|---|---|
| GCIPLT (μm) | 82.1 (0.4)^ | 68.8 (1.7)** | −1.8 (−2.3, −1.4) | 78.3 (0.7)* | −0.60 (−0.8, −0.4) |
| RNFLT (μm) | 92.8 (0.6)^ | 78.6 (2.0)** | −1.4 (−1.7, −1.0) | 90.9 (1.0) | −0.2 (−0.4, 0.02) |
| MfVEP amp | 0.61 (0.02)† | 0.40 (0.02)** | −1.4 (−1.8, −0.9) | 0.56 (0.01)* | −0.4 (−0.8, −0.03) |
| Latency (ms) | 0.7 (0.5)† | 9.5 (1.5)** | 1.1 (0.6, 1.5) | 3.9 (0.7)* | 0.5 (0.1, 0.9) |
| CS (log unit) | 1.61 (0.01)† | 1.38 (0.04)** | −1.1 (−1.6, −0.6) | 1.61 (0.01) | 0 (−0.4, 0.4) |
| HVF MD (dB) | −0.02 (0.14)§ | −2.9 (0.5)** | −1.1 (−1.6, −0.6) | −1.6 (0.2)* | −0.9 (−1.4, −0.5) |

GCIPLT: ganglion cell-inner plexiform layer thickness, RNFLT: retinal nerve fiber layer thickness, MfVEP amp: multifocal visual evoked potential amplitude measured as log signal-noise ratio, CS: contrast sensitivity, HVF: Humphrey visual field 24-2/30-2, MD: mean deviation.
Normative values from those with similar ages (mean ages all within 10 years of our MS patients') were based on † our lab controls (Laron et al., 2009, Narayanan et al., 2015b), § Wall et al. (2013), ^ Mwanza et al. (2011a).
** Statistically different from normal or non-ON ($p < 0.0001$ for all except $p = 0.02$ for HVF MD ON vs non-ON).
* Statistically different from normal ($p < 0.0001$ for GCIPLT, HVF MD; $p = 0.02$ for MfVEP amp, 0.0003 for Latency).
Cohen's d shows the standardized difference in the mean from that of normal.
Log denotes to $\log_{10}$.

**Table 3**
Percentage of eyes defined as abnormal.

| | GCIPLT[§] | RNFLT[§] | TRNFLT[§] | GCIPLT/RNFLT | Amp[†] | Lat[†] | Amp/Lat | CS[^] |
|---|---|---|---|---|---|---|---|---|
| ON | 60% | 52% | 44% | 69% | 60% | 57% | 77% | 40% |
| Non-ON | 19% | 11% | 13% | 22% | 24% | 30% | 45%[*] | 9% |

GCIPLT: ganglion cell-inner plexiform layer thickness, RNFLT: retinal nerve fiber layer thickness, TRNFLT: temporal RNFLT, Amp: multifocal visual evoked potential amplitude, Lat: multifocal visual evoked potential latency, CS: contrast sensitivity.
[*] In non-ON, more eyes showed abnormality on mfVEP (45%) than OCT (22%, $p < 0.0005$).
[^] Based on < 5% of our lab normal (Narayanan et al., 2015b).
[§] Abnormal when <5% of the age-matched machine-norm.
[†] Abnormal based on our previously established 'cluster criteria' for the probability plots (95% specificity) (Laron et al., 2009).

**Table 4**
Pearson correlation ($p$ value) between structural and functional tests.

| | ON eyes | | Non-ON eyes | |
|---|---|---|---|---|
| | GCIPLT | RNFLT[§] | GCIPLT | RNFLT[§] |
| *MfVEP Amplitude* | | | | |
| Central 5.6° | 0.78[†*] (<0.0001) | 0.43 (0.004) | 0.50 (<0.0001)[*] | 0.36 (0.002) |
| Global | 0.76[†*] (<0.0001) | 0.58[*] (<0.0001) | 0.51 (<0.0001) | 0.35 (0.003) |
| *MfVEP Latency* | | | | |
| Central 5.6° | −0.49 (0.003) | −0.34 (0.04) | −0.24 (0.04) | −0.32 (0.006) |
| Global | −0.40 (0.01) | −0.33 (0.04) | −0.29 (0.01) | −0.31 (0.007) |
| Pelli-Robson CS | 0.70 (<0.0001) | 0.61 (<0.0001) | 0.34 (0.004) | 0.47 (<0.0001) |
| 24-2/30-2 RVS | 0.45 (0.006) | 0.27 (0.11) | 0.03 (0.83) | 0.10 (0.45) |
| 10-2 RVS | 0.59 (0.03) | 0.14 (0.63) | 0.05 (0.88) | 0.18 (0.62) |

MfVEP: multifocal visual evoked potential, CS: contrast sensitivity, RVS: Humphrey visual field relative visual sensitivity, GCIPLT: ganglion cell-inner plexiform layer thickness, RNFLT: retinal nerve fiber layer thickness.
[†] Statistically different from the corresponding correlation with RNFLT in the same group ($p < 0.001$ for central, 0.01 for global after Bonferroni correction).
[§] Temporal RNFLT used for correlation with mfVEP central 5.6° and 10-2 RVS, average RNFLT used for others.
[*] Statistically different ($p < 0.05$) from the corresponding correlation with MfVEP Latency only before Bonferroni correction.

both in MS eyes past the acute stage of ON (>6 months) and those without a history of ON. Compared to RNFLT, GCIPLT measurements are less confounded by acute inflammation and edema. Studies tracking GCIPLT and RNFLT changes following an acute ON with OCT showed earlier thinning in GCIPLT (one month) than RNFLT (three months) (Huang-Link et al., 2015, Kupersmith et al., 2016). Kupersmith et al. (2016) reported that within one to two months of ON onset, 50% and 10% of their study eyes showed thinner than normal (below the 5th percentile of normal controls) GCIPLT and RNFLT, respectively; which increased to 57% and 50%, respectively, at 3 months. In some eyes, RNFL edema may take much longer to completely resolve (Huang-Link et al., 2015). In the current study, abnormal GCIPLT occurred more frequently than abnormal RNFLT: 8% more in ON > 6 months ($p = 0.33$), 7% more in non-ON ($p = 0.06$). Despite not reaching statistical significance, this difference agrees with our previous finding in a larger population of RRMS patients that significantly more eyes had abnormal GCIPLT than RNFLT (82% vs 72% in 97 eyes with ON > 6 months, $p = 0.007$; 27% vs 16% in 149 non-ON eyes, $p = 0.004$) (Narayanan et al., 2014). Similarly Gonzalez-Lopez et al reported the rate of abnormal GCIPLT vs RNFLT as 69.4% vs 55.6% in ON > 6 months, 38.5% vs 27.9% in non-ON (Gonzalez-Lopez et al., 2014).

The relationship between structural and functional deficits in RRMS is complicated by the presence of clinical or subclinical inflammation, demyelination, remyelination, neuronal and/or axonal degeneration, potential neuronal-compensatory mechanisms as well as the sensitivity/reliability of tests used. In the Kupersmith study (Kupersmith et al., 2016), visual acuity and perimetric mean deviation were not correlated with GCIPL and RNFL thickness or thinning at 6 months after ON onset; which they attributed to the need for more sensitive measurements of visual function or to redundant neural network in the macula. The current study revealed significant structure-function correlation in ON and non-ON eyes using two sensitive functional measurements: mfVEP (amplitude particularly, and latency) and CS. HVF RVS also showed a moderate correlation with GCIPLT in ON eyes, which were not observed for RNFLT. Notably, mfVEP amplitude showed stronger correlation with GCIPLT than RNFLT in ON eyes. Previous studies that included both ON (30–40%) and non-ON MS eyes also reported visual function (high and low contrast visual acuities) correlating more strongly with GCIPLT than RNFLT (Saidha et al., 2011, Seigo et al., 2012). However, this was not observed by Sriram et al. (2014) who included only non-ON eyes, and studied correlations between mfVEP amplitude/latency and GCIPLT/RNFLT. Interestingly, in our non-ON group, structure-function correlations also were not different for GCIPLT and RNFLT.

The strength of structure-function correlation is affected by many factors such as sample size, data range (disease severity), topographic mapping, and measurement variability. When comparing correlations in the same group of subjects as in the current study, measurement variability plays an important role. Peripapillary RNFLT was reported to show larger inter-subject variability due to anatomical variation of optic nerve head morphology, blood vessels, glia tissues (Hood et al., 2010) as well as worse reproducibility compared to GCIPLT (Mwanza et al., 2010, Mwanza et al., 2011b). Comparative studies of GCIPLT and RNFLT in glaucoma patients have demonstrated that macular visual sensitivity is better correlated with GCIPLT (Na et al., 2012, Shin et al., 2013). In MS eyes, RNFLT measurements are further complicated by subclinical edema and gliosis (Green et al., 2010). As suggested by delayed mfVEP or tVEP latencies, subclinical demyelination may occur in about one-third of MS eyes without a history of ON (Laron et al., 2009, Naismith et al., 2009).

A previous mfVEP study in post-acute ON reported a correlation of 0.90 between RNFLT and amplitude, −0.66 between RNFLT and latency (Klistorner et al., 2008a). It is generally believed that prolonged VEP latency reflects demyelination, as suggested in a rat model of lysolecithin-induced optic nerve demyelination (You

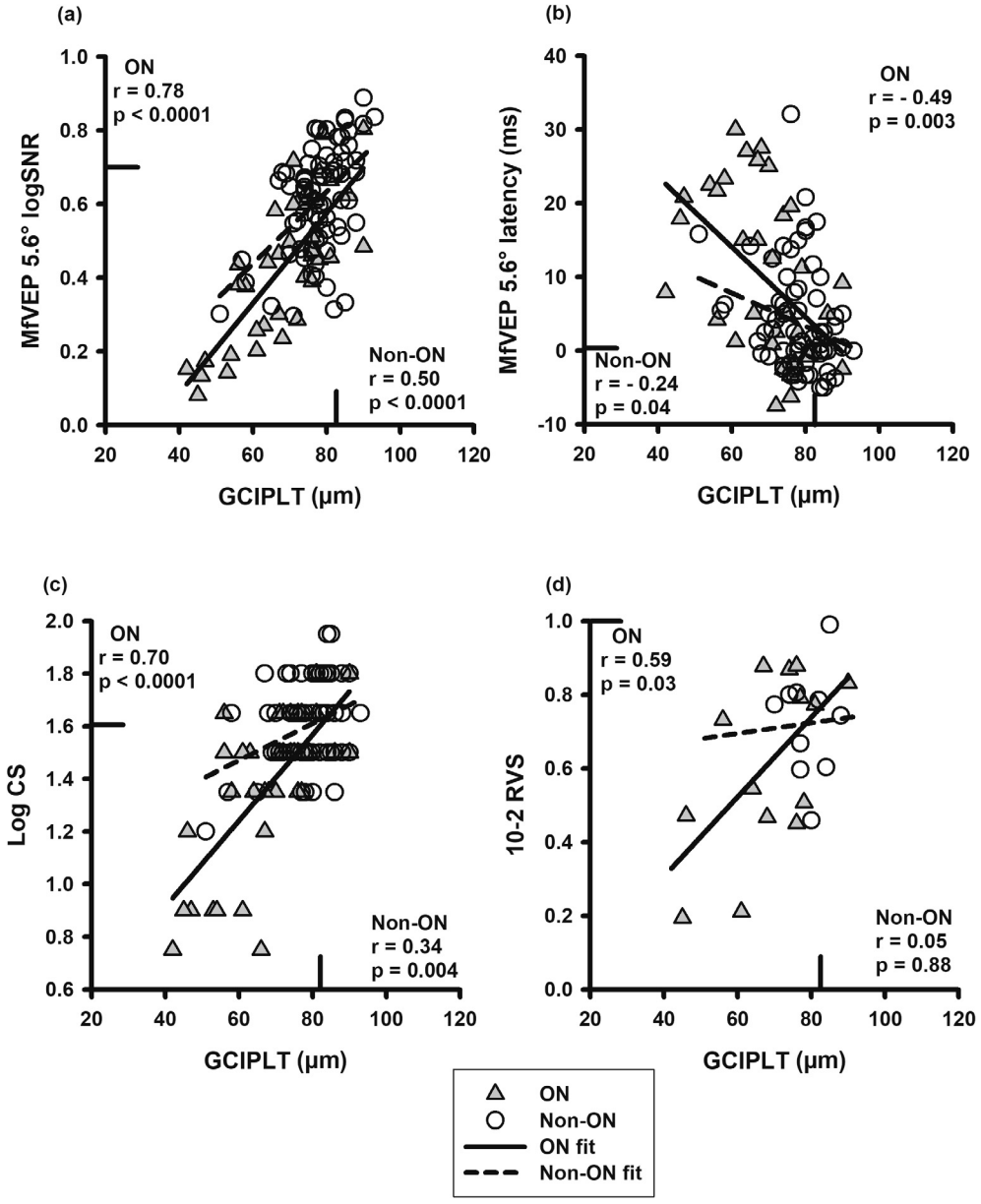


**Fig. 2.** Scatter plots illustrating correlations between ganglion cell-inner plexiform layer thickness (GCIPLT) and functional measurements in ON (filled triangles) and non-ON eyes (open circles). (a) GCIPLT vs central mfVEP amplitude (logSNR), (b) GCILPT vs central mfVEP latency, (c) GCIPLT vs CS (log units), (d) GCILPT vs 10-2 RVS. The solid and dashed lines are fitted linear regression lines for ON and non-ON eyes, respectively. The tick marks on the X and Y axis indicate previously established normative values (see Table 2). In ON eyes, mfVEP amplitude showed stronger correlation with GCIPLT ($r$ = 0.78, 0.76 for central and global amplitude) than RNFLT ($r$ = 0.43, 0.58 in Fig. 3; $p$ < 0.001, 0.01 after Bonferroni correction for central and global amplitude).

et al., 2011) whereas reduced amplitude reflects retinal ganglion cell/axonal loss. However, amplitude, latency and structural changes are intricately related. Greater demyelination (longer latency) may lead to more axonal degeneration due to lack of metabolic and trophic support. On the other hand, latency recovery (remyelination) and subclinical demyelination could compromise the correlation between latency and structural measures. In the current study, latency correlated with OCT measurements, however, such correlation was no longer significant after controlling for the effect of mfVEP amplitude.

It is well established that CS and low-contrast letter chart are more sensitive than high contrast acuity in detecting visual deficits in MS/ON and both correlate strongly with RNFLT (Fisher et al., 2006, Longbrake et al., 2016, Balcer et al., 2017). The Pelli-Robson CS chart uses large letters with a fixed size (2.8° at 1 meter) but descending contrasts, allowing CS to be measured in eyes with impaired vision. A recent study reported that 98% of MS eyes with residual visual deficits from ON could read at least two triplets of letters on the Pelli-Robson chart but more than half of them could not read any letters on the 2.5% low contrast letter chart (floor effect) (Longbrake et al., 2016). The good correlation observed between CS and structural measures (GCIPLT and RNFLT) in the current study further supports the clinical utility of Pelli-Robson chart in MS/ON eyes.

One limitation of the current study was the lack in MS EyeCARE clinic charts of Expanded Disability Status Scale (EDSS) scores which were shown by some studies to inversely correlate with OCT measurements in MS patients (Petzold et al., 2010, Britze et al., 2017). However, all of our patients (RRMS) were fully ambulatory without obvious disability noted during the exam. For the 11

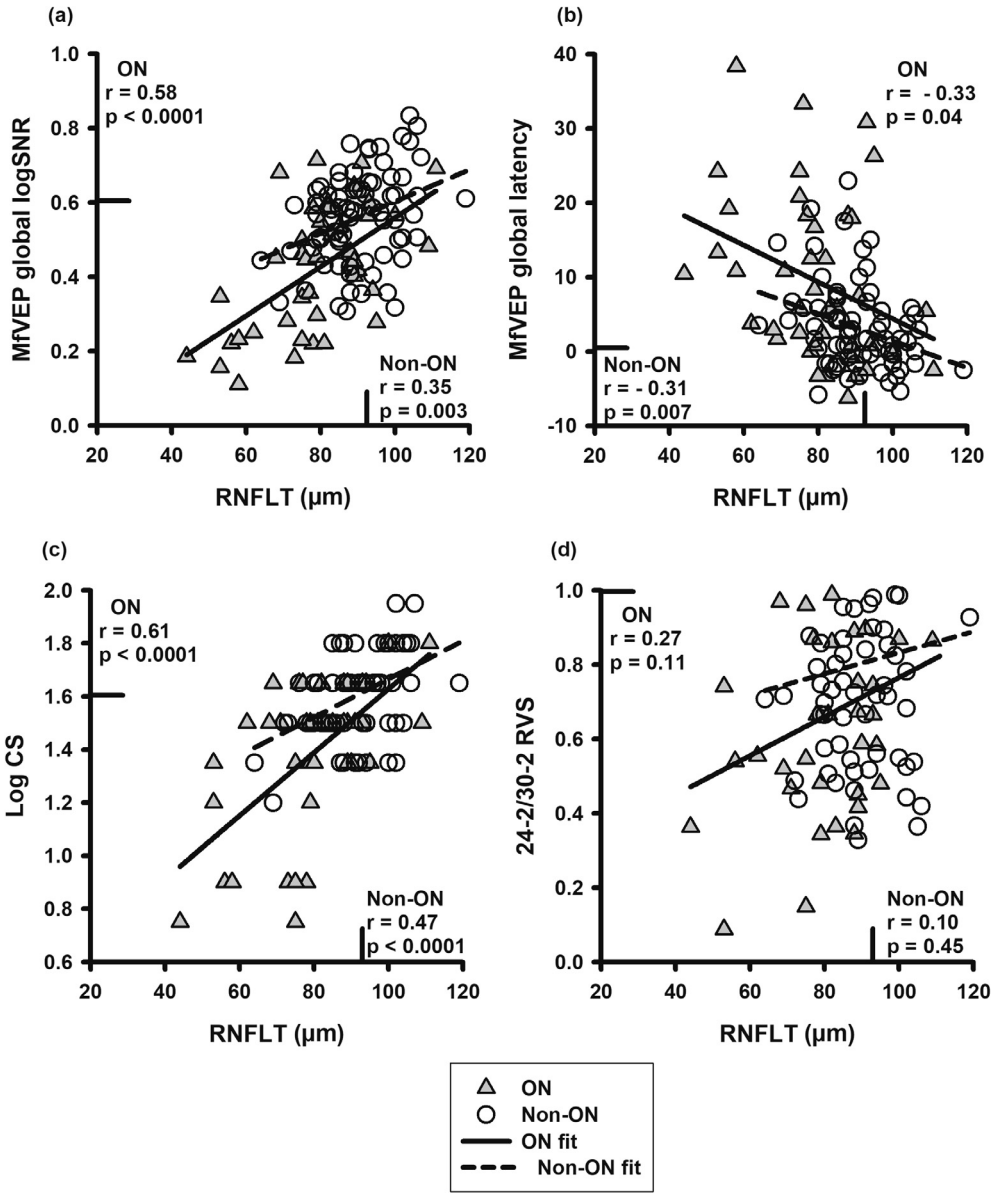


**Fig. 3.** Scatter plots illustrating correlations between retinal nerve fiber layer thickness (RNFLT) and functional measurements in ON (filled triangles) and non-ON eyes (open circles). (a) RNFLT vs mfVEP global amplitude (logSNR), (b) RNFLT vs mfVEP global latency, (c) RNFLT vs CS (log units), (d) RNFLT vs 24-2/30-2 RVS. The solid and dashed lines are fitted linear regression lines for ON and non-ON eyes, respectively. The tick marks on the X and Y axis indicate previously established normative values (see Table 2).

patients who had EDSS scores in the charts, all were less than 3. Given these observations, we estimate that most of our RRMS patients had an EDSS below 3–3.5. The statistical outcome for measurement differences between ON, non-ON and normal eyes as shown in Table 2 did not change when analyses were limited to the 28 patients who had ON in one eye and non-ON in the other eye.

Ali et al. (2014) studied 72 RRMS (mean EDSS score 3.53 ± 1.04 SD) and 13 progressive MS (mean EDSS 5.90 ± 1.43) subjects, and reported better performance of multifocal objective pupil perimetry in detecting abnormal pupillary functions in those with more severe MS: AUC 0.75 for patients with average EDSS score of 3.5, 0.92 for those with EDSS > 5. We previously performed detailed analysis of diagnostic performances of mfVEP (74 RRMS and 50 normal subjects) in detecting ON and established cluster criteria that yielded a 95% specificity and 91% sensitivity (AUC 0.96) (Laron et al., 2009). Subsequently in a group of MS patients (67 RRMS, two secondary progressive MS) who underwent both mfVEP and Stratus OCT, we found that mfVEP and RNFLT detected 89% vs 62% of ON eyes as abnormal (Laron et al., 2010). In the current study, 77% vs 52% of ON eyes were found abnormal by mfVEP vs RNFLT. We do not know whether the 10% reduction in both sensitivities was related to severity of the disease, however, the current average RNFLT is slightly thicker (by 4 μm in ON and 3 μm in non-ON) than those in our previous study after converting stratus to Cirrus OCT values (Chiselita et al., 2016). OCT performance in the current study is clearly improved by the addition of GCIPLT: GCIPLT alone detected 60% and combining GCIPLT/RNFLT detected 69% of ON as abnormal.

In the present study non-ON eyes, mfVEP performed significantly better than OCT, detecting abnormality in 23% more eyes. The mfVEP signals as we recorded using the fast pattern-reversal stimuli are considered to largely originate from the primary visual cortex (Slotnick et al., 1999, Fortune and Hood, 2003) thus could reveal demyelination in regions beyond the optic nerve including optic radiations that may not have led to structural defects at the

retinal level (Graham and Klistorner, 2017). Additionally, the diagnostic performance and recording time of mfVEP could be potentially improved by using sparse multifocal stimuli (Ruseckaite et al., 2005, Fortune et al., 2009, Maddess and Lueck, 2017).

## 5. Conclusions

In the current study, mfVEP amplitude, latency and CS showed good correlation with structural measurements in ON and non-ON eyes. MfVEP amplitude correlated more strongly with GCIPLT than RNFLT in ON eyes. Taken together with previous reports of earlier measurable thinning of GCIPLT than RNFLT in acute ON, our study supports the use of GCIPLT as a structural biomarker, mfVEP and CS as functional readouts to reflect optic nerve integrity in RRMS. MfVEP revealed more defects in non-ON eyes than OCT, demonstrating its unique value in RRMS.

## Acknowledgements

The study received supports from NIH P30 EY07551, Fight for Sight Summer Student Fellowship 2011, Minnie Flaura Turner Memorial Fund for Impaired Vision Research 2012.

## Conflict of interest

Drs. Narayanan, Cheng, and Frishman report no disclosures. Dr. Tang has received research funds from Quark lab, River Vision, Horizon Pharma and Novartis and is a speaker for EMD Serono, Sanofi, Mallinckrodt, and Teva.

## References

Ali EN, Maddess T, James AC, Voicu C, Lueck CJ. Pupillary response to sparse multifocal stimuli in multiple sclerosis patients. Mult Scler 2014;20:854–61.
American Clinical Neurophysiology Society. Guideline 5: guidelines for standard electrode position nomenclature. Am J Electroneurodiag Technol 2006;46:222–5225.
Balcer LJ, Raynowska J, Nolan R, Galetta SL, Kapoor R, Benedict R, et al. Validity of low-contrast letter acuity as a visual performance outcome measure for multiple sclerosis. Mult Scler 2017;23:734–47.
Britze J, Pihl-Jensen G, Frederiksen JL. Retinal ganglion cell analysis in multiple sclerosis and optic neuritis: a systematic review and meta-analysis. J Neurol 2017;264:1837–53.
Brusa A, Jones SJ, Kapoor R, Miller DH, Plant GT. Long-term recovery and fellow eye deterioration after optic neuritis, determined by serial visual evoked potentials. J Neurol 1999;246:776–82.
Cheng H, Laron M, Schiffman JS, Tang RA, Frishman LJ. The relationship between visual field and retinal nerve fiber layer measurements in patients with multiple sclerosis. Invest Ophthalmol Vis Sci 2007;48:5798–805.
Chiselita D, Pantalon AD, Cantemir A, Galatanu C. Translating data and measurements from stratus to cirrus OCT in glaucoma patients and healthy subjects. Rom J Ophthalmol 2016;60:158–64.
Costello F, Hodge W, Pan YI, Eggenberger E, Coupland S, Kardon RH. Tracking retinal nerve fiber layer loss after optic neuritis: a prospective study using optical coherence tomography. Mult Scler 2008;14:893–905.
Drasdo N, Millican CL, Katholi CR, Curcio CA. The length of Henle fibers in the human retina and a model of ganglion receptive field density in the visual field. Vision Res 2007;47:2901–11.
Fisher JB, Jacobs DA, Markowitz CE, Galetta SL, Volpe NJ, Nano-Schiavi ML, et al. Relation of visual function to retinal nerve fiber layer thickness in multiple sclerosis. Ophthalmology 2006;113:324–32.
Fortune B, Demirel S, Bui BV. Multifocal visual evoked potential responses to pattern-reversal, pattern-onset, pattern-offset, and sparse pulse stimuli. Vis Neurosci 2009;26:227–35.
Fortune B, Hood DC. Conventional pattern-reversal VEPs are not equivalent to summed multifocal VEPs. Invest Ophthalmol Vis Sci 2003;44:1364–75.
Fortune B, Zhang X, Hood DC, Demirel S, Johnson CA. Normative ranges and specificity of the multifocal VEP. Doc Ophthalmol 2004;109:87–100.
Gonzalez-Lopez JJ, Rebolleda G, Leal M, Oblanca N, Munoz-Negrete FJ, Costa-Frossard L, et al. Comparative diagnostic accuracy of ganglion cell-inner plexiform and retinal nerve fiber layer thickness measures by Cirrus and Spectralis optical coherence tomography in relapsing-remitting multiple sclerosis. Biomed Res Int 2014;2014 128517.
Graham SL, Klistorner A. Afferent visual pathways in multiple sclerosis: a review. Clin Exp Ophthalmol 2017;45:62–72.
Green AJ, McQuaid S, Hauser SL, Allen IV, Lyness R. Ocular pathology in multiple sclerosis: retinal atrophy and inflammation irrespective of disease duration. Brain 2010;133:1591–601.
Grover LK, Hood DC, Ghadiali Q, Grippo TM, Wenick AS, Greenstein VC, et al. A comparison of multifocal and conventional visual evoked potential techniques in patients with optic neuritis/multiple sclerosis. Doc Ophthalmol 2008;117:121–8.
Hood DC, Greenstein VC. Multifocal VEP and ganglion cell damage: applications and limitations for the study of glaucoma. Prog Retin Eye Res 2003;22:201–51.
Hood DC, Ohri N, Yang EB, Rodarte C, Zhang X, Fortune B, et al. Determining abnormal latencies of multifocal visual evoked potentials: a monocular analysis. Doc Ophthalmol 2004a;109:189–99.
Hood DC, Salant JA, Arthur SN, Ritch R, Liebmann JM. The location of the inferior and superior temporal blood vessels and interindividual variability of the retinal nerve fiber layer thickness. J Glaucoma 2010;19:158–66.
Hood DC, Zhang X, Rodarte C, Yang EB, Ohri N, Fortune B, et al. Determining abnormal interocular latencies of multifocal visual evoked potentials. Doc Ophthalmol 2004b;109:177–87.
Huang-Link YM, Al-Hawasi A, Lindehammar H. Acute optic neuritis: retinal ganglion cell loss precedes retinal nerve fiber thinning. Neurol Sci 2015;36:617–20.
Klistorner A, Arvind H, Nguyen T, Garrick R, Paine M, Graham S, et al. Axonal loss and myelin in early ON loss in postacute optic neuritis. Ann Neurol 2008a;64:325–31.
Klistorner A, Fraser C, Garrick R, Graham S, Arvind H. Correlation between full-field and multifocal VEPs in optic neuritis. Doc Ophthalmol 2008b;116:19–27.
Kupersmith MJ, Garvin MK, Wang JK, Durbin M, Kardon R. Retinal ganglion cell layer thinning within one month of presentation for optic neuritis. Mult Scler 2016;22:641–8.
Laron M, Cheng H, Zhang B, Schiffman JS, Tang RA, Frishman LJ. Assessing visual pathway function in multiple sclerosis patients with multifocal visual evoked potentials. Mult Scler 2009;15:1431–41.
Laron M, Cheng H, Zhang B, Schiffman JS, Tang RA, Frishman LJ. Comparison of multifocal visual evoked potential, standard automated perimetry and optical coherence tomography in assessing visual pathway in multiple sclerosis patients. Mult Scler 2010;16:412–26.
Longbrake EE, Lancia S, Tutlam N, Trinkaus K, Naismith RT. Quantitative visual tests after poorly recovered optic neuritis due to multiple sclerosis. Mult Scler Relat Disord 2016;10:198–203.
Maddess T, Lueck CJ. Multiple sclerosis seen through new eyes. Clin Exp Ophthalmol 2017;45:9–11.
Maghzi AH, Minagar A, Waubant E. Neuroprotection in multiple sclerosis: a therapeutic approach. CNS Drugs 2013;27:799–815.
Mwanza JC, Chang RT, Budenz DL, Durbin MK, Gendy MG, Shi W, et al. Reproducibility of peripapillary retinal nerve fiber layer thickness and optic nerve head parameters measured with cirrus HD-OCT in glaucomatous eyes. Invest Ophthalmol Vis Sci 2010;51:5724–30.
Mwanza JC, Durbin MK, Budenz DL, Girkin CA, Leung CK, Liebmann JM, et al. Profile and predictors of normal ganglion cell-inner plexiform layer thickness measured with frequency-domain optical coherence tomography. Invest Ophthalmol Vis Sci 2011a;52:7872–9.
Mwanza JC, Oakley JD, Budenz DL, Chang RT, Knight OJ, Feuer WJ. Macular ganglion cell-inner plexiform layer: automated detection and thickness reproducibility with spectral domain-optical coherence tomography in glaucoma. Invest Ophthalmol Vis Sci 2011b;52:8323–9.
Na JH, Kook MS, Lee Y, Baek S. Structure-function relationship of the macular visual field sensitivity and the ganglion cell complex thickness in glaucoma. Invest Ophthalmol Vis Sci 2012;53:5044–51.
Naismith RT, Tutlam NT, Xu J, Shepherd JB, Klawiter EC, Song SK, et al. Optical coherence tomography is less sensitive than visual evoked potentials in optic neuritis. Neurology 2009;73:46–52.
Narayanan D, Cheng H, Bonem KN, Saenz R, Tang RA, Frishman LJ. Tracking changes over time in retinal nerve fiber layer and ganglion cell-inner plexiform layer thickness in multiple sclerosis. Mult Scler 2014;20:1331–41.
Narayanan D, Cheng H, Tang RA, Frishman LJ. Longitudinal evaluation of visual function in multiple sclerosis. Optom Vis Sci 2015a;92:976–85.
Narayanan D, Cheng H, Tang RA, Frishman LJ. Reproducibility of multifocal visual evoked potential and traditional visual evoked potential in normal and multiple sclerosis eyes. Doc Ophthalmol 2015b;130:31–41.
Petzold A, Balcer LJ, Calabresi PA, Costello F, Frohman TC, Frohman EM, et al. Retinal layer segmentation in multiple sclerosis: a systematic review and meta-analysis. Lancet Neurol 2017;16:797–812.
Petzold A, de Boer JF, Schippling S, Vermersch P, Kardon R, Green A, et al. Optical coherence tomography in multiple sclerosis: a systematic review and meta-analysis. Lancet Neurol 2010;9:921–32.
Pietroboni AM, Dell'Arti L, Caprioli M, Scarioni M, Carandini T, Arighi A, et al. The loss of macular ganglion cells begins from the early stages of disease and correlates with brain atrophy in multiple sclerosis patients. Mult Scler 2017. 1352458517740214.
Pihl-Jensen G, Schmidt MF, Frederiksen JL. Multifocal visual evoked potentials in optic neuritis and multiple sclerosis: A review. Clin Neurophysiol 2017;128:1234–45.
Pisa M, Guerrieri S, Di Maggio G, Medaglini S, Moiola L, Martinelli V, et al. No evidence of disease activity is associated with reduced rate of axonal retinal atrophy in MS. Neurology 2017;89:2469–75.

Ratchford JN, Saidha S, Sotirchos ES, Oh JA, Seigo MA, Eckstein C, et al. Active MS is associated with accelerated retinal ganglion cell/inner plexiform layer thinning. Neurology 2013;80:47–54.
Ruseckaite R, Maddess T, Danta G, Lueck CJ, James AC. Sparse multifocal stimuli for the detection of multiple sclerosis. Ann Neurol 2005;57:904–13.
Saidha S, Syc SB, Durbin MK, Eckstein C, Oakley JD, Meyer SA, et al. Visual dysfunction in multiple sclerosis correlates better with optical coherence tomography derived estimates of macular ganglion cell layer thickness than peripapillary retinal nerve fiber layer thickness. Mult Scler 2011;17:1449–63.
Seigo MA, Sotirchos ES, Newsome S, Babiarz A, Eckstein C, Ford E, et al. In vivo assessment of retinal neuronal layers in multiple sclerosis with manual and automated optical coherence tomography segmentation techniques. J Neurol 2012;259:2119–30.
Shin HY, Park HY, Jung KI, Park CK. Comparative study of macular ganglion cell-inner plexiform layer and peripapillary retinal nerve fiber layer measurement: structure-function analysis. Invest Ophthalmol Vis Sci 2013;54:7344–53.
Slotnick SD, Klein SA, Carney T, Sutter E, Dastmalchi S. Using multi-stimulus VEP source localization to obtain a retinotopic map of human primary visual cortex. Clin Neurophysiol 1999;110:1793–800.
Sriram P, Wang CY, Yiannikas C, Garrick R, Barnett M, Parratt J, et al. Relationship between optical coherence tomography and electrophysiology of the visual pathway in non-optic neuritis eyes of multiple sclerosis patients. PLoS One 2014;9.
Syc SB, Saidha S, Newsome SD, Ratchford JN, Levy M, Ford E, et al. Optical coherence tomography segmentation reveals ganglion cell layer pathology after optic neuritis. Brain 2012;135:521–33.
Toosy AT, Naismith RT, Villoslada P. OCT as a window to the MS brain: the view becomes slightly clearer. Neurology 2017;89:2404–5.
Wall M, Doyle CK, Zamba KD, Artes P, Johnson CA. The repeatability of mean defect with size III and size V standard automated perimetry. Invest Ophthalmol Vis Sci 2013;54:1345–51.
Walter SD, Ishikawa H, Galetta KM, Sakai RE, Feller DJ, Henderson SB, et al. Ganglion cell loss in relation to visual disability in multiple sclerosis. Ophthalmology 2012;119:1250–7.
Wang J, Cheng H, Hu YS, Tang RA, Frishman LJ. The photopic negative response of the flash electroretinogram in multiple sclerosis. Invest Ophthalmol Vis Sci 2012;53:1315–23.
Yang EB, Hood DC, Rodarte C, Zhang X, Odel JG, Behrens MM. Improvement in conduction velocity after optic neuritis measured with the multifocal VEP. Invest Ophthalmol Vis Sci 2007;48:692–8.
You Y, Klistorner A, Thie J, Graham SL. Latency delay of visual evoked potential is a real measurement of demyelination in a rat model of optic neuritis. Invest Ophthalmol Vis Sci 2011;52:6911–8.